# EECS C145B / BioE C165: Image Processing and Reconstruction Tomography

**Lecture 12**

Jonathan S. Maltz

**This handout contains copyrighted material. It is for personal educational use only. Do not distribute.**

jon@eecs.berkeley.edu
http://muti.lbl.gov/145b
510-486-6744



## Topics to be covered

1. Introduction to single photon emission tomography (SPECT)
2. Examples of SPECT studies
3. Components of SPECT systems
   - Gantry
   - Collimators
   - Detectors
4. Scattering physics
5. Photon attenuation
6. Radiotracers
7. Image reconstruction
8. Frontiers in SPECT



## Reading

Assigned reading:

- Reader pp. 105-151

### Optional reading

- Webb, "The Physics of Medical Imaging", Institute of Physics Publishing (1998), pp. 11-12, 142-193, 221-244, 256-318.
- Sandler et al., "Diagnostic Nuclear Medicine", Third Edition, Williams & Wilkins, Vol. I, pp. 1-7, 9-25, 47-57, 67-79 81-92, 121-138 (1996).
- Shung et al., "Principles of Medical Imaging", Academic Press, pp. 164-212 (1992).
- Cho, "Foundations of Medical Imaging", John Wiley and Sons (1993), pp. 165-200.



## Introduction to SPECT

Single photon emission computed tomography involves imaging of radioactive source distributions **within** a body given measurements of the photons **emitted by these sources** taken **outside** the body. A computer is used to reconstruct the imaged distribution.

- SPECT is usually used to image **injected radiotracer** compounds for the purpose of evaluating biological function. These agents are called **radiopharmaceuticals.**
- In SPECT, the nuclei of the injected radioisotope decay to produce gamma photons. Each such nuclear decay yields a **single photon**.
- Gamma photons easily penetrate living tissue, but are subject to attenuation and scatter.
- **Contrast** in SPECT is based on the **differential concentration** of the radionulcide in space.

## Introduction to SPECT

Photograph courtesy Marconi Corp.

State-of-the art SPECT system with three camera heads mounted on a rotating gantry. These heads rotate around the subject. Transaxial sections may be imaged in this way.



## Applications of single photon imaging: Thyroid function

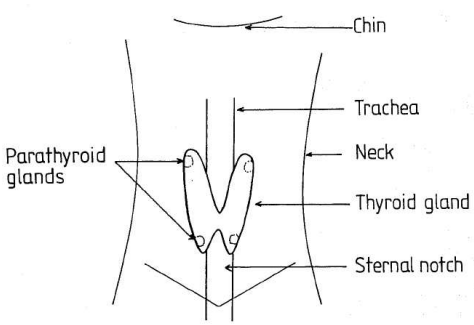


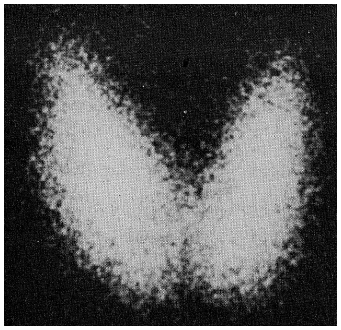

Source: Webb, p. 295

Single photon planar scinitigraph of thyroid gland. The tracer $^{99m}$Tc-pertechnetate is trapped in the functioning thyroid.



## Applications of single photon imaging: Thyroid function

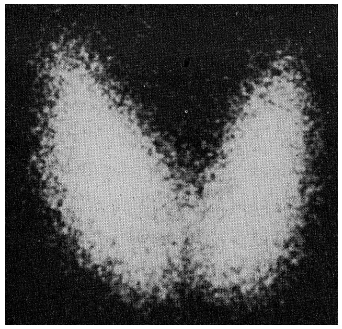

Normal thyroid

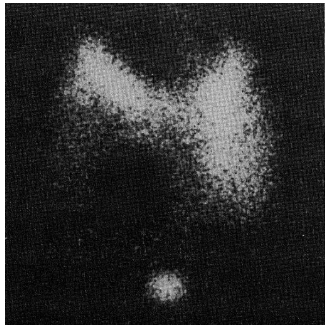

Follicular thyroid cancer

Source: Webb, p. 295-6



## Applications of single photon imaging: Thyroid function

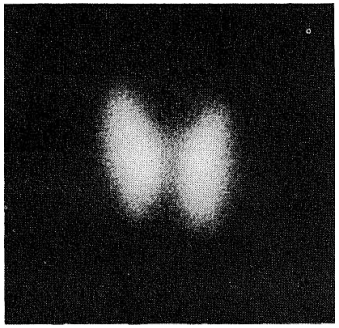

Graves' disease

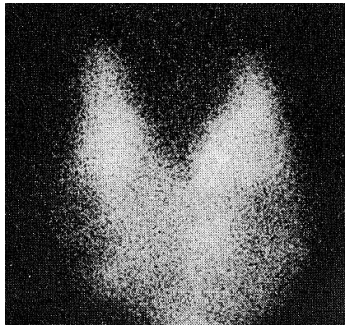

Plummer's disease

Source: Webb, p. 295

In both Graves' disease and Plummer's disease, thyroid function is elevated (hyperthyroidism). The left figure shows uniformly increased thyroid function. The right figure shows massive thyroid enlargement (goiter). The tracer used was $Na^{131}I$.

## Applications of SPECT: Cardiac function

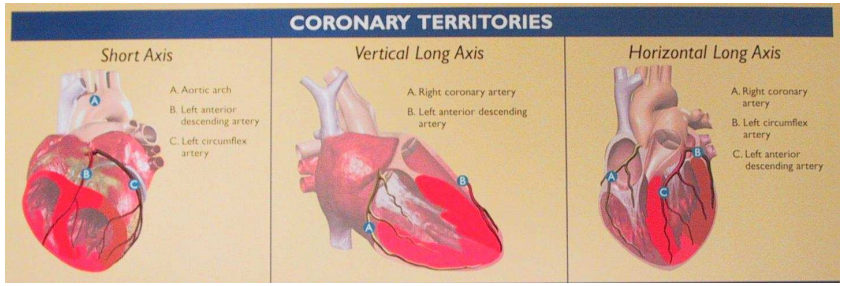


Source: Webb, p. 295-6

Imaging of the cardiac muscle (myocardium) is the most common study performed in human nuclear medical imaging. Usually, tracers are employed that are deposited in the muscle in proportion to the flow rate of blood through the muscle.



## Applications of SPECT: Cardiac function

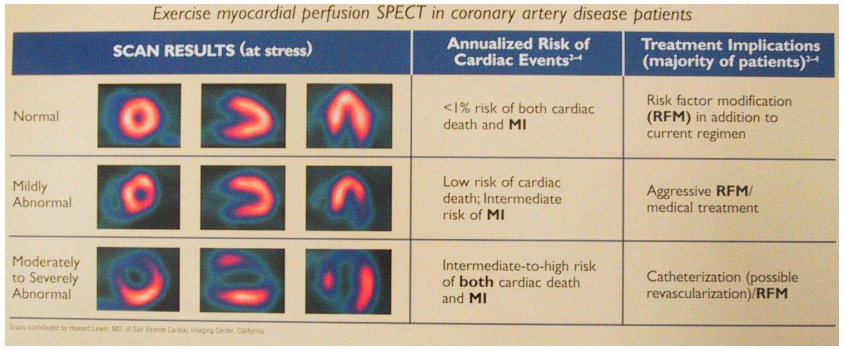

*Exercise myocardial perfusion SPECT in coronary artery disease patients*

| SCAN RESULTS (at stress) | | | | Annualized Risk of Cardiac Events[3–4] | Treatment Implications (majority of patients)[3–4] |
|---|---|---|---|---|---|
| Normal | | | | <1% risk of both cardiac death and **MI** | Risk factor modification **(RFM)** in addition to current regimen |
| Mildly Abnormal | | | | Low risk of cardiac death; Intermediate risk of **MI** | Aggressive **RFM**/ medical treatment |
| Moderately to Severely Abnormal | | | | Intermediate-to-high risk of **both** cardiac death and **MI** | Catheterization (possible revascularization)/**RFM** |

Scans contributed by Howard Lewin, MD, of San Vicente Cardiac Imaging Center, California

Source: Cardiolite promotional material

After exercise, blood flow in all areas of the myocardium is high in normal hearts. Heart muscle death (following a heart attack) or narrowing of the coronary arteries (stenosis) eliminate or reduce flow, and hence tracer deposition. Hypoperfused muscle appears darker than healthy muscle.



## Applications of SPECT: Neuroimaging

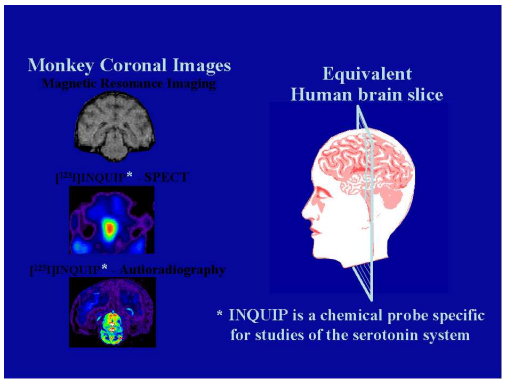


Source: DNMFI, LBNL

The middle image in the left column shows the **binding** of a tracer that attaches to the serotonin transporter. SPECT yields a lower resolution image compared to the autoradiograph image (below), which is produced by physically slicing the brain and placing it on radiation-sensitive film. Why? _____



## Components of SPECT systems

The components necessary for SPECT imaging are:

1. A rotating gantry, or a mechanism to rotate the subject in front of the camera.
2. A gamma camera to detect incoming photons.
3. Analog circuitry: amplifiers, pulse shapers and counters.
4. A digital computer and reconstruction algorithm.
5. An isotope to inject.

## Components of SPECT systems: Rotation mechanism

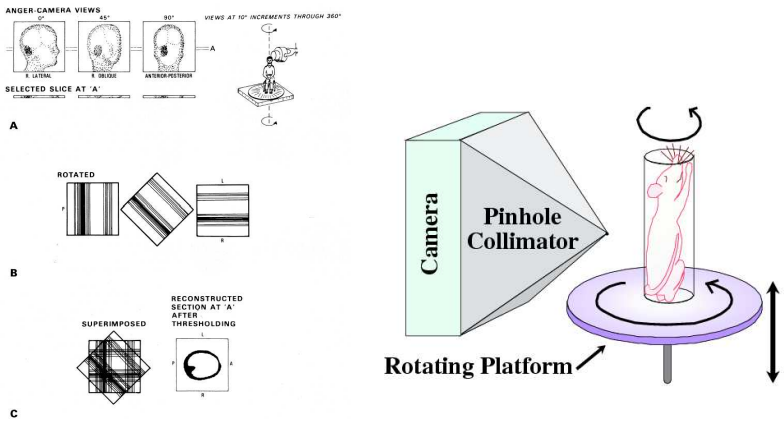


Source: Budinger, LBNL

In the first implementation of quatitative SPECT, Budinger and Gullberg rotated a patient in front of a gamma camera and used Fourier and iterative reconstruction algorithms to reconstruct the source distribution. This approach has found renewed application in some modern experimental small animal imaging systems.



## Components of SPECT systems: Rotation mechanism

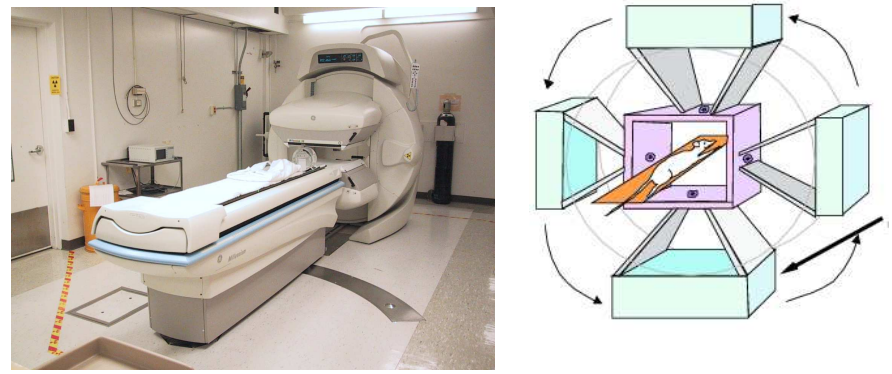

Source: Budinger, LBNL (right)

Most SPECT instruments mount the gamma camera(s) on a rotating **gantry**.



## Components of SPECT systems: Gamma camera

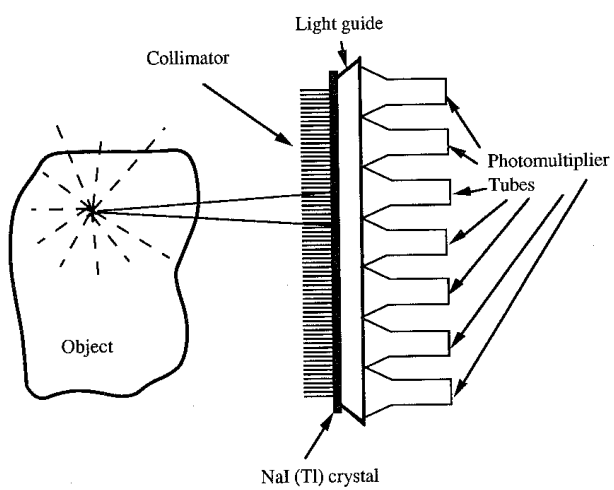


Source: Cho, p. 166



## Components of SPECT systems: Gamma camera

Most gamma cameras consist of:

1. A lead or tungsten **collimator** that accepts into a projection bin only those photons traveling toward that bin in a certain direction. This is important if the measurements are to represent line integrals of activity.
2. A layer of scintillator crystal that emits visible light when struck by gamma photons. The **higher the energy** of the incident gamma, the **larger the number** of visible photons that are produced.
3. A light guide that directs visible light produced inside the scintillator to visible light detectors (classically, photomulitplier tubes).
4. A layer of photomulitplier tubes (PMTs) that detects incident light photons and produces a current proportional to the energy of the incident gamma.

## Components of SPECT systems: Collimator: Pinhole

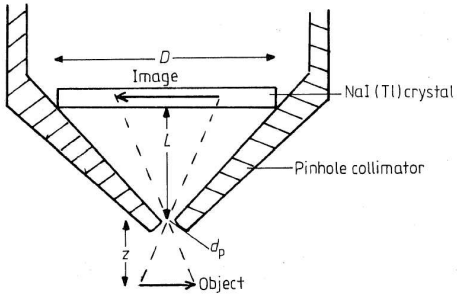


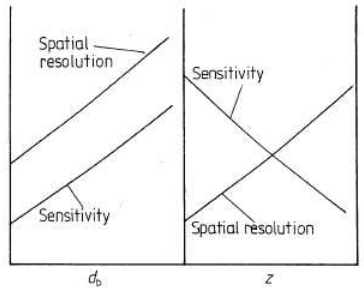


Source: Webb p. 164-5

The smaller the pinhole of a pinhole collimator, the larger the scinitillator and the closer the source, the greater is the resolving power of the camera. However, the sensitivity of the camera decreases as pinhole diameter and source distance are increased. How should "spatial resolution" be interpreted in the diagram on the right? _____



## Components of SPECT systems: Collimator: Converging

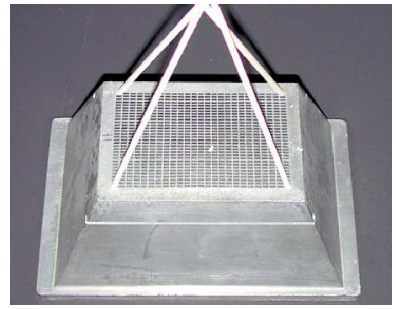

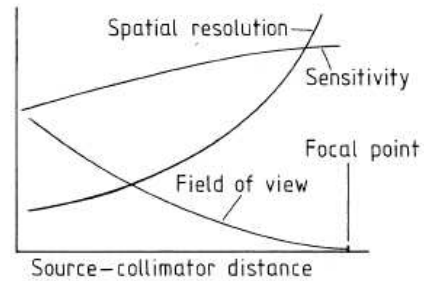


Source: Budinger, LBNL (left), Webb p. 165 (right)

A converging hole collimator has its highest sensitivity and highest resolution at its focal point. It is useful for imaging small regions. In the graph on the right, "spatial resolution" must be interpreted as resolving power.



## Components of SPECT systems: Collimator: Converging

Detector Arrangement

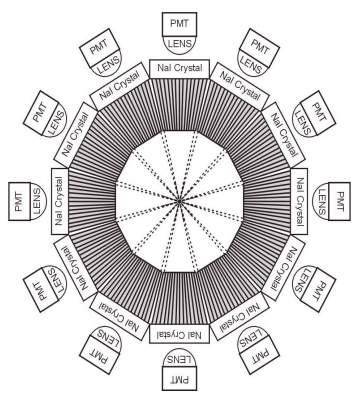


Centered

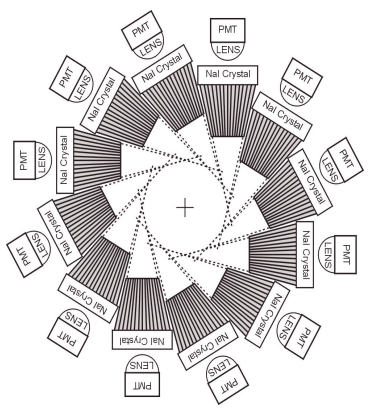


In Motion



## Components of SPECT systems: Collimator: Diverging

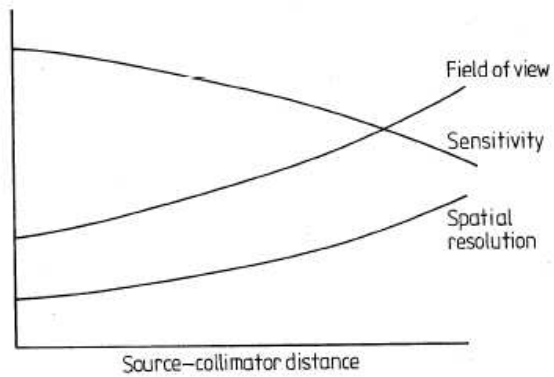


Source: Webb p. 165

A diverging hole collimator provides larger field-of-view at the expense of resolution and sensitivity. In the graph on the right, "spatial resolution" must be interpreted as resolution in units of distance (e.g. millimeters).

## Components of SPECT systems: Gamma camera: Collimator: Parallel hole

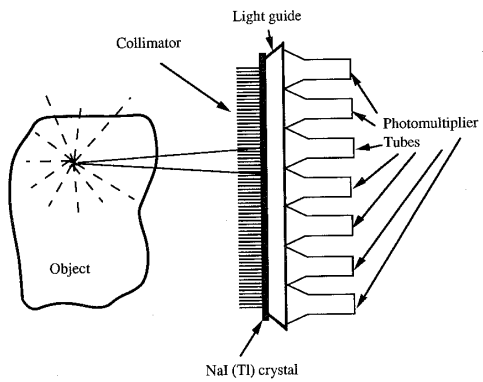


Source: Cho, p. 166

The parallel collimator is the most popular choice for general imaging. It offers uniform resolution over its field of view and does not introduce geometric distortion.



## Components of SPECT systems: Gamma camera: Scintillator layer

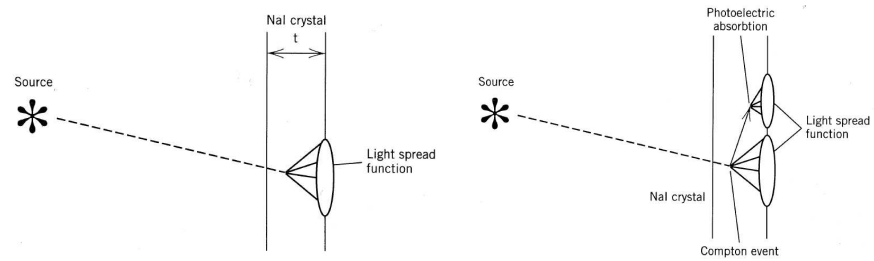


Source: Cho, p. 169.

The scintillator layer is made out of a crystal that has a high electron density (atomic number). This increases its photon stopping power. When a gamma is stopped, many visible light photons are released. The thicker the scintillator layer, the greater its stopping power (sensitivity), but the wider is the point spread function associated with the event. Resolution is lowered in this way owing to the spread of light as it travels from the position of the event to the detector surface (at the right edge). Compton scatter (which we discuss later) also leads to widening of the PSF and loss of spatial resolution.



## Components of SPECT systems: Gamma camera: PMTs

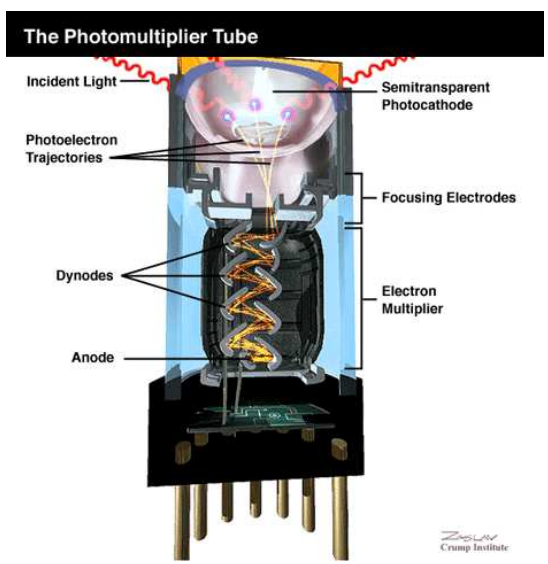


Source: Crump Institute, UCLA.



## Components of SPECT systems: Gamma camera: PMTs

- A set of photomulitplier tubes (PMT) is attached to the scinitillator surface.
- PMTs detect incident light photons.
- When a visible light photon exits the scintillator and strikes the photocathode of the PMT, a loosely bound electron in the thin film of the photocathode is dislodged 15-30% of the time. An electron that has been knocked out in this way is called a **photoelectron.** The probability of dislodging an electron is termed the **quantum efficiency** of the photocathode. The photocathode is usually made out of an alloy of cesium and antimony.
- Each photoelectron accelerates towards the first dynode, which is typically held at a potential of 300V above that of the cathode.
- When the electron hits the dynode, it knocks out about four other electrons. These electrons in turn accelerate towards the second dynode, which is held at 600V with respect to the cathode

## Components of SPECT systems: Gamma camera: PMTs

- Most PMTs have between 6 and 14 dynode stages. Gains of $10^5$-$10^8$ are realized. A current in the anode circuit of the PMT flows to neutralize the accumulation of charge on the anode.
- The **magnitude of the anode circuit current** is proportional to the **energy of the incident photon**.
- The anode is connected to the highest voltage supply (1000V) using a load resistor. The voltage across this resistor is, by Ohm's Law, directly proporitonal to the electron current flowing out of the anode. It is hence proportional to the energy of the original incident gamma.
- Each gamma that interacts with the photocathode thus produces a **voltage pulse** at the load resistor.



## Components of SPECT systems: Gamma camera: PMTs

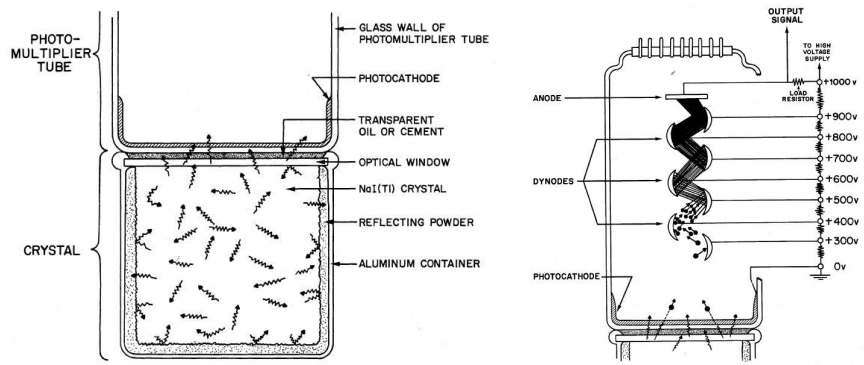


Source: Webb, p. 49

The left figure shows 3 eV photons created within the scinitillator crystal by an incident gamma. Only photons directed towards the photocathode of the PMT can exit. The remainder are reflected. The right figure illustrates the amplification of photoelectrons in a PMT.



## Components of SPECT systems: Gamma camera: PMTs

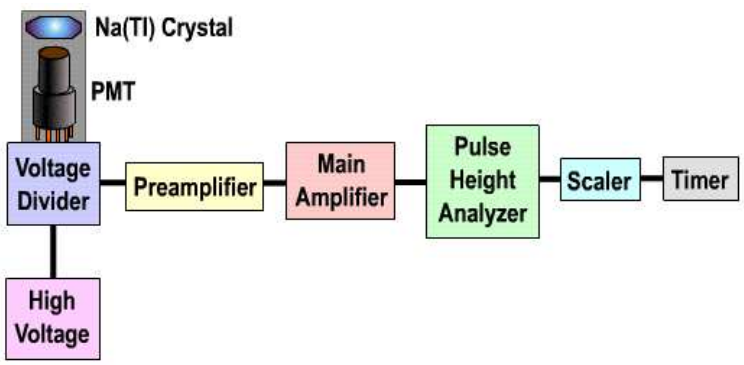


Source: Gambhir, UCLA.

Analog electronics is used to amplify, shape and count the voltage pulses from the PMT.



## Components of SPECT systems: Gamma camera: PMTs

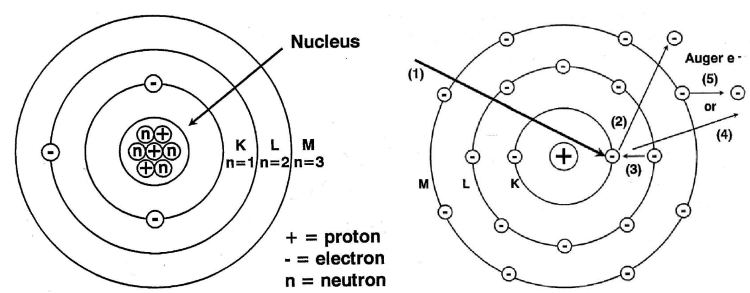


Source: Sandler, p. 9. Right diagram modified.

The left figure shows a simplified model of the atom. The nucleus is surrounded by the K, L and M shells. The right figure illustrates the **creation of a photoelectron** by an incident gamma photon. The visible light photon (1) hits an inner shell electron (2), which is ejected. An outer shell electron (3) then fills this hole. Excess energy is released as a light photon of lower energy (4) or an Augér electron (5).

## Components of SPECT systems: Gamma camera: PMTs

- If we record the output of a PMT over a finite time interval, we can plot the number of events as a function of pulse height. This is called the **pulse height spectrum**. It is a histogram of the energy distribution of the incident gammas.
- Having good **energy resolution** in this spectrum is essential if the system is to **reject scattered gamma photons**. These have lower energy than unscattered gammas.
- Photodiodes and other semiconductor detectors have replaced PMTs in some modern designs. Individual semiconductor materials have advantages over PMTs in terms of cost, size, spatial resolution and energy resolution. However, each material has its shortcomings. Some semiconductor detectors can directly stop gammas, and so obviate the need for a separate scintillator. Solid-state detectors may, within a few years, be able to replace PMTs, just as transistors have largely replaced the thermionic vacuum tube in electronics.



## Components of SPECT systems: Gamma camera: Pulse height spectra

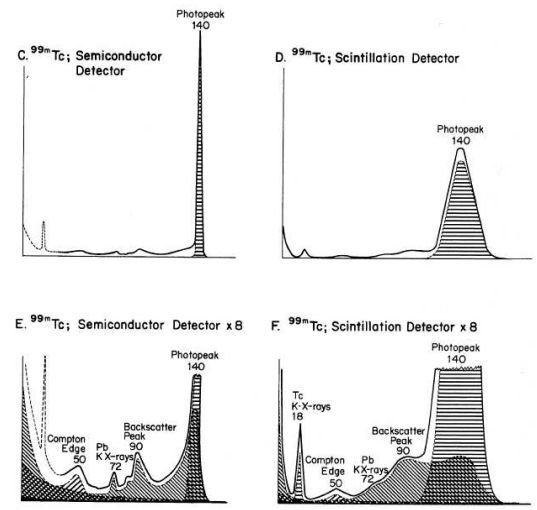


Source: Webb, p. 52



## Components of SPECT systems: Gamma camera: Pulse height spectra

Referring to diagram on previous page:

- Pulse height spectra are shown for $^{99m}$Tc. The amplitude is given in terms of energy in keV.
- Graphs E and F are eight times magnifications of C and D, respectively.
- The upper solid line is the observed spectrum.
- The dashed lines are the theoretical spectra given an ideal detector.
- Horizontal crosshatch: totally absorbed photos.
- Heavy diagonal crosshatch: partially absorbed primary photons.
- Light diagonal crosshatch: predetector-scattered photons.
- Lower solid line: background photons.



## Components of SPECT systems: Gamma camera: Pulse height spectra

- Photopeak: Energy at which the maximum number of photons was detected.
- Compton edge: maximum energy a scattered photon transfers to scintillator crystal (single Compton event).
- Backscatter peak: Minimum energy of a predector-scattered photon after one interaction (Compton scatted of 180 degrees)
- Lead K x-rays arise from gamma interaction within the lead collimator.

To understand what these peaks in the spectrum represent, we must study gamma photon scattering phenomena.

## Gamma ray physics: Scatter: Compton scatter

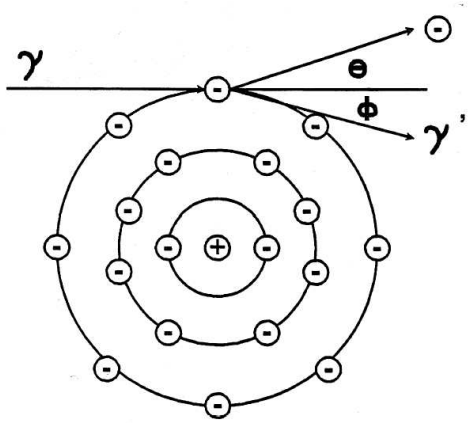


Source: Sandler, p. 24

In a Compton interaction, an incident gamma hits an outer shell electron. Energy is transferred to the electron, which is scattered at angle $\theta$. The gamma alters its direction of travel by the angle $\phi$.



## Gamma ray physics: Scatter: Compton scatter

- By conservation of energy:

$$E_\gamma = E'_\gamma + E_e$$

where $E_e$ is the energy of the recoil electron.

- Considering also the conservation of momentum we have:

$$E'_\gamma = \frac{E_\gamma}{1 + (E_\gamma / 511\text{keV})(1 - \cos(\phi))}$$

where 511keV is the rest mass of the electron.

- When $\phi = 0$, degrees, there is no interaction and $E'_\gamma = E_\gamma$
- When $\phi = 180$ degrees, there is backscatter and $E'_\gamma$ is minimized.
- Compton interaction is the dominant mode of scatter in living tissues in medical imaging.



## Gamma ray physics: Scatter: Compton scatter

*Energy of Scattered Photon (γ) and Scattered Electron ($e^-$) vs. Scattering Angle in Compton Scattering*

| Photon Energy[a] (keV) | Scattering Angle 0° γ | 0° $e^-$ | 30° γ | 30° $e^-$ | 45° γ | 45° $e^-$ | 90° γ | 90° $e^-$ | 180° γ | 180° $e^-$ |
|---|---|---|---|---|---|---|---|---|---|---|
| 70 | 70 | 0 | 69 | 1 | 67 | 3 | 62 | 8 | 55 | 15 |
| 140 | 140 | 0 | 135 | 5 | 130 | 10 | 110 | 30 | 90 | 50 |
| 364 | 364 | 0 | 332 | 32 | 301 | 63 | 213 | 151 | 150 | 214 |
| 511 | 511 | 0 | 451 | 60 | 395 | 116 | 255 | 256 | 170 | 341 |

[a]Primary photon energies of $^{201}$Tl, $^{99m}$Tc, $^{131}$I, and annihilation radiation respectively.

Source: Sandler, p. 24



## Gamma ray physics: Scatter: Photoelectric absorbtion

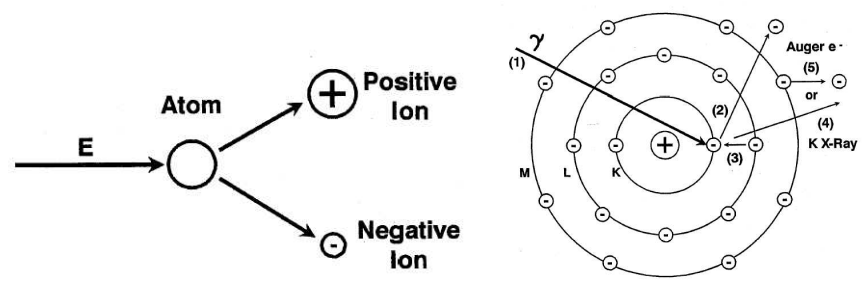


Source: Sandler, p. 23

The process of photoelectric absorbtion in living tissues is the same as that which occurs at the photocathode of a PMT. It involves the interaction of a gamma with an inner shell electron, the ejection of the electron, and the production of a K x-ray when an electron in an outer shell fills the resulting hole and releases the energy of the bandgap.

## Gamma ray physics: Scatter in diagnostic nuclear medicine

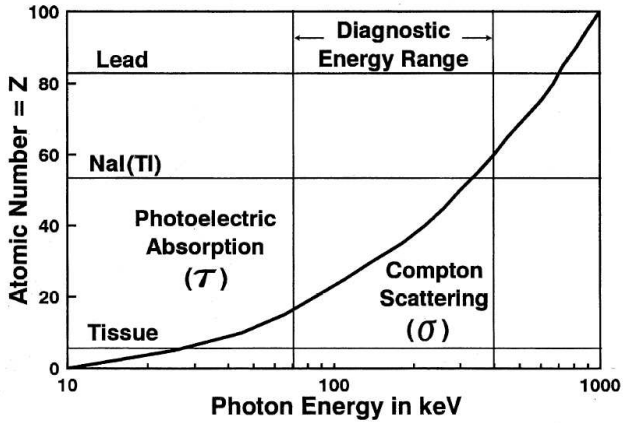


Source: Sandler, p. 23

Left of the solid line, photoelectric absorbtion dominates. To the right of this line, Compton scattering is more probable.



## Scattering in SPECT

- In SPECT, a large number of the counts detected are scattered events.
- The most effective way to reject scatter is to set an **energy window** that accepts only those events with an energy close to the photopeak energy of the isotope being used.
- Usually, an energy window of $15 - 20\%$ is chosen.
- For example, the radionuclide $^{99m}$Tc has a photopeak at 140 keV. A scanner with a 15% window will discard the events associated with all photons whose energy is below 119 keV.
- The greater the **energy resolution** of the detector, the more effectively scattered photons are rejected. A typical energy resolution is 10% for a PMT-based camera.
- Why can't we set the window to a width of say 1%?



## Scattering in SPECT

- Usually, two side-by-side windows are used. We have already discussed the high energy (photopeak) window. The low energy window is used to estimate the number of scattered photons that contribute to counts in the photopeak window.
- A fraction of this estimate is subtracted from the counts in the photopeak window.
- Scatter compensation has also been attempted where an algorithm deconvolves an average scatter linespread function from the data. This approach is prone to error. Why?



## Scattering in SPECT

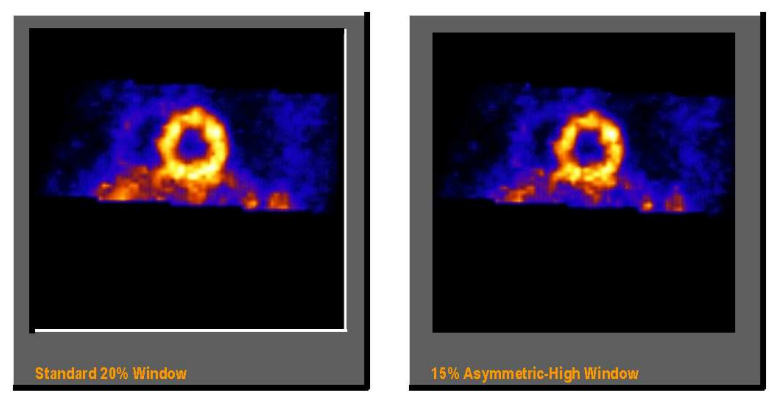


Image courtesy Marconi Corp.

The myocardial perfusion SPECT image on the left was acquired using a 20% energy window. The image on the right was reconstructed from events within 15% of the photopeak energy. Scatter artifact to the bottom left of the myocardium is reduced through the use of a narrower window.

## Attenuation in SPECT

- In x-ray CT, attenuation is the source of contrast.
- In emission imaging, attenuation is an unwanted complication:
  1. It makes the reconstruction problem **non-linear**: the projections are not the Radon transform of the source distribution.
  2. It decreases the number of observed events and hence the signal-to-noise ratio (SNR). The administered radiation dose must also be larger than would be required in the absence of attentuation.
  3. Projections 180 degrees apart are **no longer identical.** Projections must thus be acquired over a **full 360 degrees.**



## Attenuation compensation

- In order to accurately compensate for attenuation, we need to know the attenuation coefficients at all points in the distribution. This map can be generated using x-ray CT imaging.
- When at iterative reconstruction algorithm is used, we may proceed as follows:
  1. Project our current guess of the emission distribution into projection space. This requires a modified projection operator that accounts for the attenuation at each point through which the source ray traverses.
  2. Using an ML method or otherwise, obtain a measure of how well our projections fit the data. Calculate the gradient of this goodness-of-fit cost function.
  3. Modify the image pixel values by taking a step that has a component in the direction opposite to the gradient. This will reduce the cost.
  4. Return to Step 1 unless the cost function fails to decrease over several iterations.



## Attenuation compensation

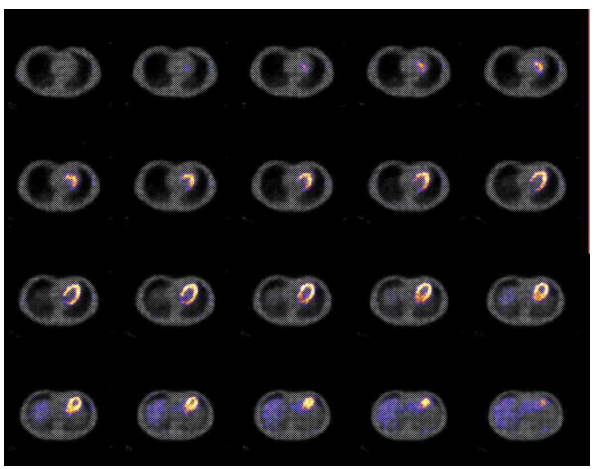

Image courtesy Marconi Corp.

Attenuation-corrected myocardial perfusion SPECT study overlaid on the corresponding x-ray CT attenuation map.



## Attenuation compensation

- Because iterative algorithms are slow compared to convolve-backproject type methods, they have not until recently enjoyed much use in clinical SPECT.
- Approximate methods were developed that, for example, weight each reconstructed image pixel value with the average attenuation experienced by rays intersecting that pixel.
- These and related methods are not quantitative and will not be discussed in detail. Their importance will diminish further as computational power becomes cheaper. See Cho pp. 176-178 for details.

## Attenuation compensation

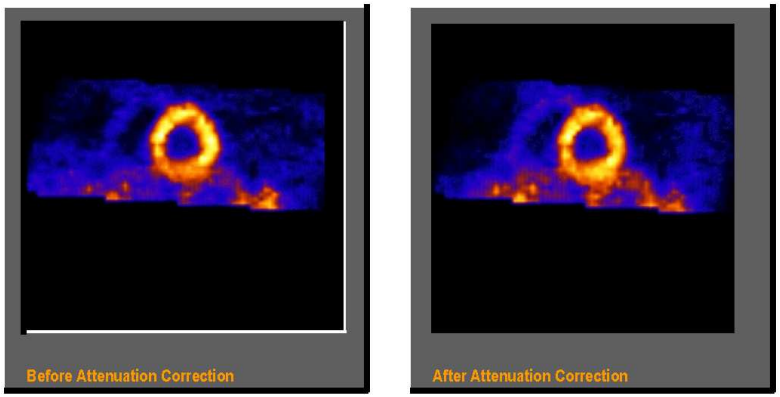


Image courtesy Marconi Corp.

The effects of attenuation are most pronounced in the inferior myocardium, which is furthest from the camera. We observe an artifact there that suggests a perfusion defect. After attenuation correction, this artifact disappears.



## Radiotracers for SPECT

Characteristics of important radionuclides

| Element | Radionuclide | Emission | Photon energy (MeV) | Half-life |
|---|---|---|---|---|
| Carbon | $^{11}C$ | $e^+$ | 0.511 | 20 min |
| Nitrogen | $^{13}N$ | $e^+$ | 0.511 | 10 min |
| Oxygen | $^{15}O$ | $e^+$ | 0.511 | 124 sec |
| Fluorine | $^{18}F$ | $e^+$ | 0.511 | 109 min |
| Cobalt | $^{57}Co$ | $\gamma$ | 0.122, 0.136 | 270 days |
| Gallium | $^{68}Ga$ | $\gamma$ | 0.511, 1.077 | 68 min |
| Technetium | $^{99m}Tc$ | $\gamma$ | 0.14 | 6 hrs |
| Indium | $^{113m}In$ | $\gamma$ | 0.393 | 102 min |
| Iodine | $^{123}I$ | $\gamma$ | 0.159 | 13 hrs |
| Iodine | $^{131}I$ | $\gamma$ | 0.080, 0.284, 0.364 | 8 days |
| Thallium | $^{201}Tl$ | $\gamma$ | 0.135, 0.167 | 73 hrs |

Source: Shung p. 165

Although positron ($e^+$) emitters may be used for SPECT, lower energy radionuclides are far more commonly employed.



## Radiotracers for SPECT

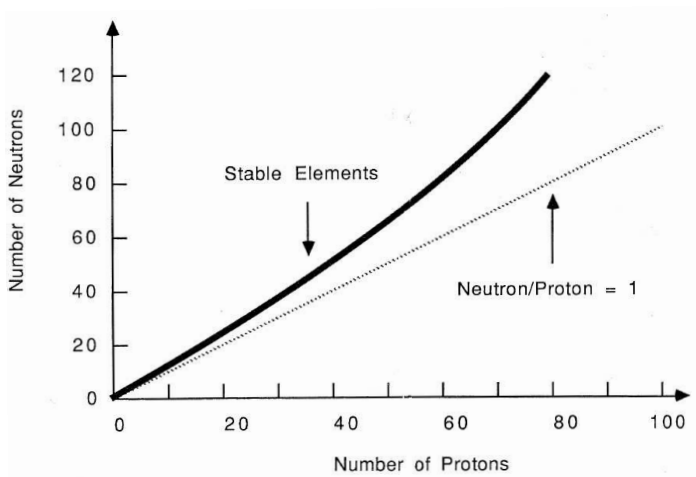


Source: Sandler p. 13

Unstable isotopes have an unfavorable neutron/proton ($N/Z$) ratio and fall above or below the line of stability.



## Radiotracers for SPECT

- All important SPECT isotopes exhibit $\beta$ and/or positron and/or electron capture decay.
- $\beta$ decay occurs in nuclei that have an unfavorably high neutron to proton ratio (N/Z).
- In $\beta$ decay, a nucleus of element $X$ having atomic number $Z$ and atomic weight $A$ decays according to the equation:

$$^{A}_{Z}X \rightarrow ^{A}_{Z+1}Y + \beta^- + \nu + Q$$

  where $\beta^-$ is an electron that originates in the nucleus, $\nu$ is a neutrino and $Q$ is excess energy.
- This equation can also be written as:

$$^{1}_{0}n \rightarrow ^{1}_{1}p + \beta^- + \nu + Q$$

  where $p$ is a proton.

## Radiotracers for SPECT

- Emitted $\beta^-$ particles have energies that range from zero to $Q$.
- When $E_\beta = Q$, no gamma ray is emitted.
- The average $E_\beta \approx 1/3\,Q$.
- An antineutrino $\bar{\nu}$ carries off the excess energy when $E_\beta < Q$.
- After $\beta$ decay, gamma rays may be emitted from the nucleus as it rearranges into a stable configuration.
- An example of $\beta$ decay is the transformation of ${}^{131}_{53}\mathrm{I}$:

$$ {}^{131}_{53}\mathrm{I} \rightarrow {}^{131}_{54}\mathrm{Xe} + \beta^- + \bar{\nu} $$



## Radiotracers for SPECT

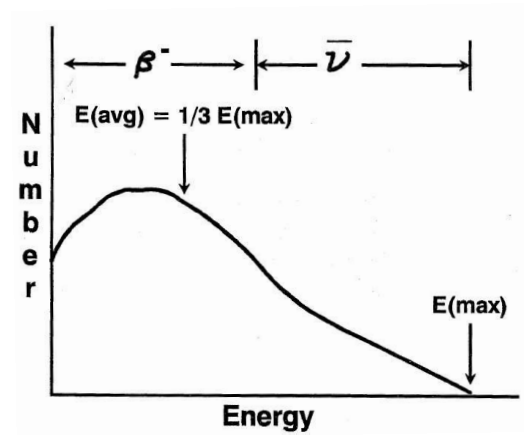


Source: Sandler p. 13

Emitted $\beta^-$ particles have a continuous energy range. Excess energy is carried away by an antineutrino, which has no mass and no charge.



## Radiotracers for SPECT

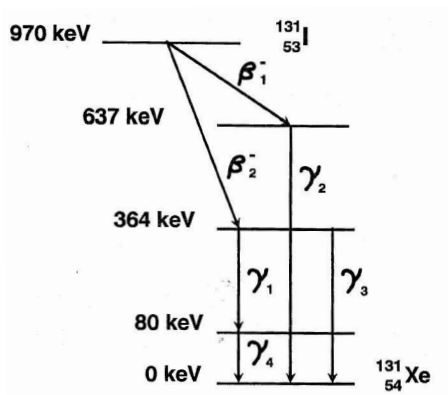


Source: Sandler p. 13

The decay of ${}^{131}_{53}\mathrm{I}$ into ${}^{131}_{54}\mathrm{Xe}$ occurs via two modes of emission of $\beta^-$ particles. Gamma rays of four different energies may be released to return the nucleus to an unexcited state.



## Radiotracers for SPECT

- **Positron emission** occurs in nuclei that are unstable because they have too many protons relative to neutrons. A stable state is achieved through the decay:

$$ {}^{A}_{Z}X \rightarrow {}^{A}_{Z-1}Y + \beta^+ + \nu + Q $$

  where $\beta^+$ is a positron. It has the same mass as, but the opposite charge of, an electron.
- This equation can also be written as:

$$ {}^{1}_{1}p \rightarrow {}^{1}_{0}n + \beta^+ + \nu + Q $$

- The energy required to transform a proton into a heavier neutron is provided by other nucleons as they rearrange.
- As was the case for $\beta^-$ particles, positrons have a continuous range of energies. Excess energy is carrier off by a neutrino.

## Radiotracers for SPECT

- As soon as a positron loses its energy, it combines with an electron and **annihilates**. In this matter-antimatter reaction, the mass of the two particles is completely destroyed and converted into energy.
- Two 511 keV photons are released in opposite directions.
- An example of positron emission is the transformation of ${}^{15}_{8}\mathrm{O}$:

$$ {}^{15}_{8}\mathrm{O} \rightarrow {}^{15}_{7}\mathrm{N} + \beta^{+} + \nu $$

- Positron emitters are most commonly used in PET, although some SPECT systems can be equipped with collimators suitable for such high-energy gammas.
- What would happen if ${}^{15}_{8}\mathrm{O}$ were used on a SPECT system intended for ${}^{99\mathrm{m}}\mathrm{Tc}$?



## Radiotracers for SPECT

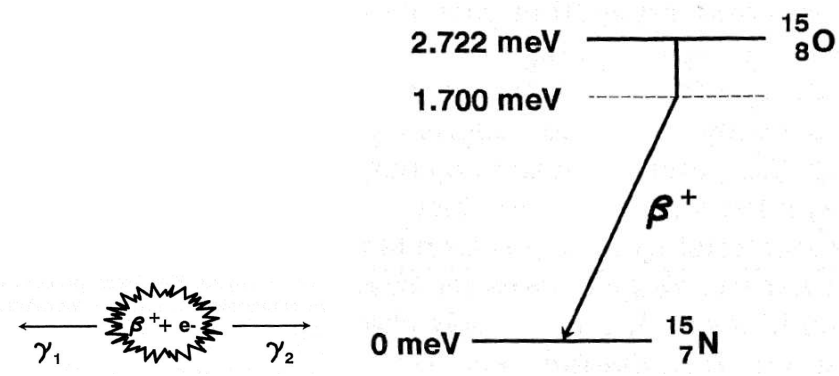


Source: Sandler p. 14

In living tissues ejected positrons annihilate with electrons within a few millimeters of the mother nucleus. Positron range is a blurring effect in SPECT and PET. Oxygen-15 has only one mode of decay - via positron emission.



## Radiotracers for SPECT

- In **electron capture**, the nucleus captures an inner shell electron. An outer shell electron fills this hole and a characteristic x-ray or Auger electron is released.

$$ {}^{A}_{Z}X + e^{-} \rightarrow {}^{A}_{Z-1}Y + \nu + Q $$

- This equation can also be written as:

$$ {}^{1}_{1}p + e^{-} \rightarrow {}^{1}_{0}n + \nu + Q $$

- Electron capture occurs in nuclei where $N/Z$ is unfavorably low.
- An example of electron capture is the transformation of ${}^{201}_{81}\mathrm{Tl}$:

$$ {}^{201}_{81}\mathrm{Tl} \rightarrow {}^{201}_{80}\mathrm{Hg} + \nu + \gamma $$

- Electron capture can be thought of as reverse beta decay. The two processes sometimes compete with each other.



## Radiotracers for SPECT

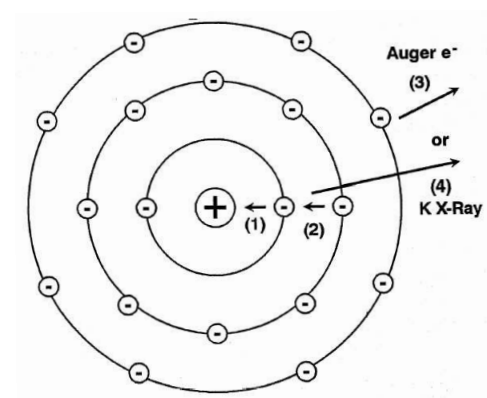


Source: Sandler p. 14

Schematic diagram of electron capture. A nucleus in an excited state disposes of its excess energy by capturing an inner shell electron.

## Radiotracers for SPECT

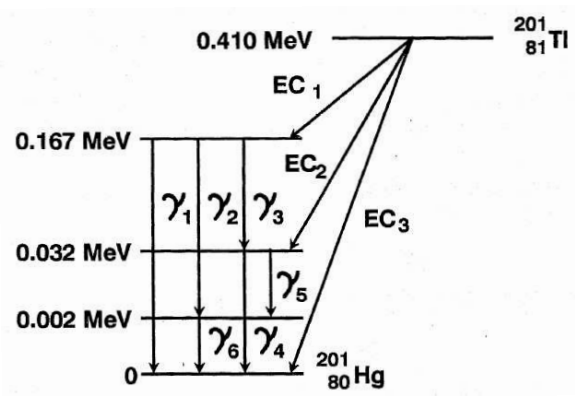


Source: Sandler p. 14

Thallium-201 can decay to mercury-201 via three electron capture processes. Gamma rays of six different energies are released.



## Radiotracers for SPECT

A nucleus that finds itself in an excited state, perhaps because of $\beta^-$ emission or electron capture, can release this energy via two processes:

1. **Gamma emission**
2. **Internal conversion**: the nucleus imparts energy to an inner shell electron, which is then ejected from the atom. An outer shell electron fills this hole and a characteristic x-ray or Auger electron is released. No gamma leaves the atom. Internal conversion can be understood in terms of the nucleus releasing a gamma and this gamma being completely absorbed by an inner shell electron. Internal conversion competes with gamma emission.
   Would an isotope with high internal conversion efficiency be desirable for imaging?



## Radiotracers for SPECT

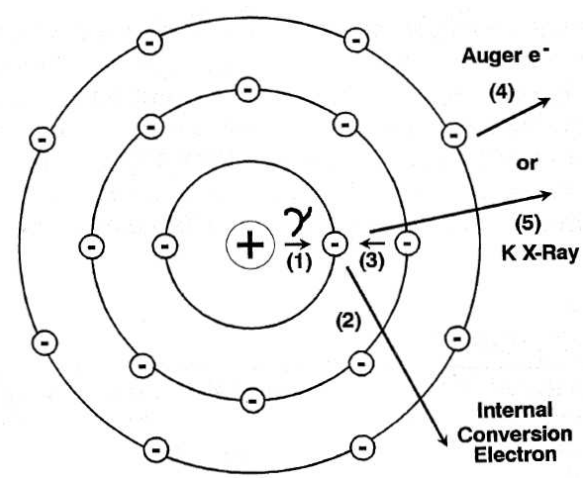


Source: Sandler p. 15

In internal conversion, a gamma released by the nucleus is absorbed by an inner shell electon. No gamma leaves the atom.



## Radiotracers for SPECT

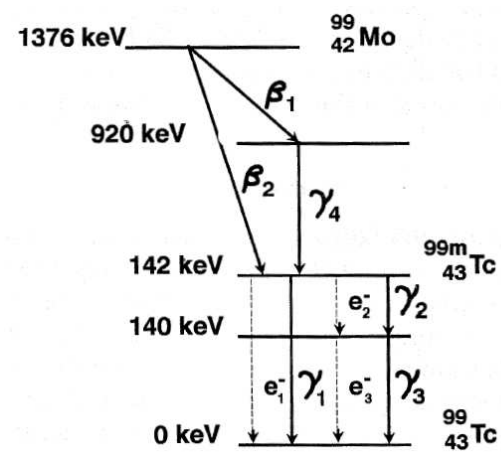


Source: Sandler p. 15

Internal conversion competes with gamma emission in the decay of the metastable isotope technetium-99m into technetium-99.

## Radiotracers for SPECT

*Table 2.5.*
*Nuclear Decay Data for Radionuclides used in Clinical Nuclear Medicine Imaging*

| Nuclide | Half-Life | Transition | Energy (keV) | Abundance (%) |
|---|---|---|---|---|
| $^{67}$Ga | 78 hrs | EC[a] (93 KeV x-rays) | 93 | 100 |
| | | Gamma 1[b] | 185 | 38 |
| | | Gamma 2[b] | 300 | 24 |
| | | Gamma 3[b] | 394 | 16 |
| | | Gamma 4 | 93 | 4 |
| | | IC[c] electron 1 | 185 | 33 |
| | | IC[c] electron 2 | 300 | <1 |
| | | IC[c] electron 3 | | <1 |
| $^{111}$In | 68 hrs | EC[a] (23 KeV x-rays) | 172 | 100 |
| | | Gamma 1[b] | 247 | 90 |
| | | Gamma 2[b] | 172 | 94 |
| | | IC[c] electron 1 | 247 | 10 |
| | | IC[c] electron 2 | | 6 |
| $^{123}$I | 13 hrs | EC[a] (27 KeV x-rays) | 159 | 98 |
| (Fig 2.12) | | Gamma[b] | 159 | 84 |
| | | IC[c] electron | 159 | 16 |
| $^{131}$I | 8 days | Beta 1 | 333 | 7 |
| | | Beta 2 | 606 | 90 |
| (Fig 2.7) | | Gamma 1 | 284 | 6 |
| | | Gamma 2 | 637 | 7 |
| | | Gamma 3[b] | 364 | 84 |
| | | Gamma 4 | 80 | 7 |
| $^{99m}$Mo | 66 hrs | Beta 1 | 456 | 18 |
| (Fig 2.13) | | Beta 2 | 1234 | 80 |
| | | Gamma 4 | 778 | 5 |
| $^{99m}$Tc | 6 hrs | Gamma 1 | 142 | <1 |
| (Fig 2.13) | | Gamma 2 | 2 | 1 |
| | | Gamma 3[b] | 140 | 88 |
| | | IC[c] electron 1 | 142 | 1 |
| | | IC[c] electron 2 | 2 | 99 |
| | | IC[c] electron 3 | 140 | 11 |
| $^{201}$Tl 100 | 73 hrs | EC[a] (70 KeV x-rays)$_{Hg}$ | | |
| (Fig 2.11) | | Gamma 1 | 167 | 10 |
| | | Gamma 3 | 135 | <3 |
| | | IC[c] electron 1 | 167 | 15 |
| | | IC[c] electron 3 | 135 | 8 |
| $^{133}$Xe | 5 days | Beta | 346 | 99 |
| | | Gamma[b] | 81 | 37 |
| | | IC[c] electron | 81 | 52 |
| $^{11}$C | 20 min | Positron[d] | 960 | 100 |
| $^{13}$N | 10 min | Positron[d] | 1198 | 100 |
| $^{15}$O | 122 sec | Positron[d] | 1732 | 100 |
| $^{68}$Ga | 68 min | Positron 1[d] | 822 | 1 |
| | | Positron 2[d] | 1899 | 88 |
| | | EC[a] (9.1 KeV x-rays) | | 11 |
| $^{18}$F | 110 min | Positron[d] | 633 | 97 |
| | | EC[a] (0.5 KeV x-rays) | | 3 |
| $^{82}$Rb | 1.3 min | Positron 1[d] | 2375 | 12 |
| | | Positron 2[d] | 3150 | 83 |
| | | EC[a] (13 KeV x-rays) | | 5 |

[a]EC = Electron Capture (characteristic radiation secondary)
[b]Transition used for imaging
[c]IC = Internal Conversion (Note! The energies stated for the internal conversion electrons include those of the resulting characteristic x-rays and/or Auger electrons.)
[d]511 keV γ-rays result from positron annihilation and are used for imaging

Source: Sandler p. 17



## Sampling in SPECT

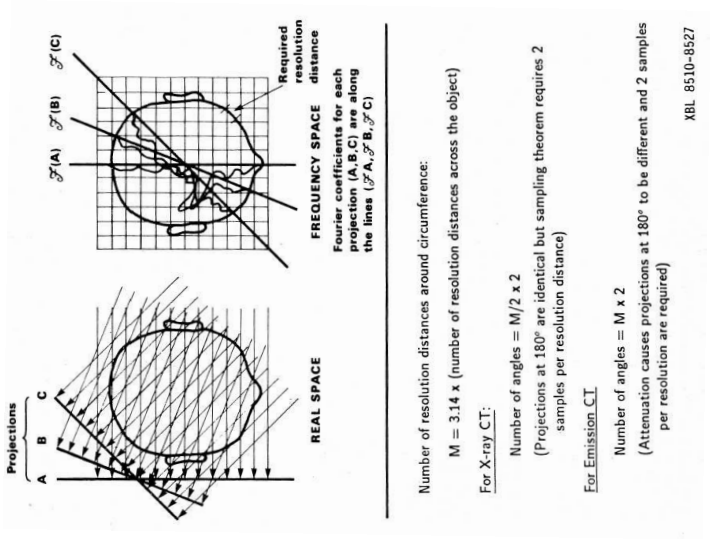


Source: Sandler p. 131



## Sampling in SPECT

Angular sampling:

- For the Radon transform, we derived an expression for the angular increment that ensures sampling above the Nyquist rate:

$$\Delta\theta < \frac{1}{\rho_{\max} D}$$

- Over $\pi$ radians, the number of projections required was:

$$N_t > \frac{\pi}{\Delta\theta} = \frac{\pi}{\rho_{\max} D}$$

If $d = 1/\rho_{\max}$ is the resolution of the imaging system, then:

$$N_t > \frac{\pi D}{d}$$

- In SPECT, we have to sample the distribution over $2\pi$ radians. So

$$N_e > \frac{2\pi D}{d}$$

This is identical to the expression given on the previous page.

Radial sampling: expression identical to that derived for the Radon transform.



## Reconstruction of SPECT images

- When we derived the filter-backprojection class of algorithms, we found that we could reconstruct the imaged distribution by deconvolving the backprojection image and the PSF of the Radon transform.
- When attenuation is present, the backprojection operator is not appropriate: we can't smear the same projection value back across the whole image (This conflicts with physical reality).
- If we backproject, while accounting for attenuation, the PSF at each point in the image will, in general, be unique. A different inverse filter must be applied to each point.
- Consequently, the filter-backprojection algorithms are not appropriate, as they specify that a ramp filter be applied to the entire backprojection image.

## Reconstruction of SPECT images

- The projection operator, however, can be modified to take attenuation into account when an attenuation map is available.
- Image reconstruction can be accomplished by:
  1. Repeatedly executing the **forward problem** by projecting the current estimate of the source distribution **through** the attenuation map.
  2. Correcting the source distribution estimate to make its projections **fit the measured projection data better.**



## Reconstruction of SPECT images

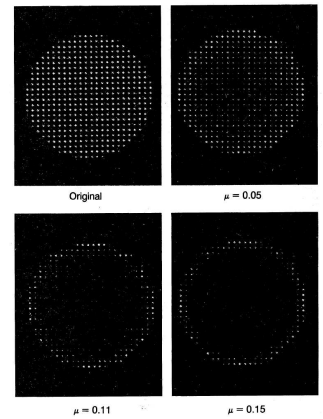


Source: Sandler p. 128

The effects of attenuation on reconstruction when algorithms that do not account for attenuation are employed. $\mu = 0.11$ and $\mu = 0.15$ correspond to the average attenuation coefficients of 511keV and 140keV gammas in tissue, respectively.



## Frontiers of SPECT: Dynamic SPECT

- When we reconstruct a CT or SPECT image, we assume that all of the data we acquire are projections of the same attenuation/source distribution.
- Most SPECT systems have a slowly rotating single camera head that takes minutes to acquire a complete set of projections.
- If the radiotracer redistributes significantly during the imaging period, **inconsistent projections** result.
- Under these conditions, we are effectively imaging many different distributions and taking a single projection of each.
- This is consequently a **highly underdetermined** problem.



## Frontiers of SPECT: Dynamic SPECT

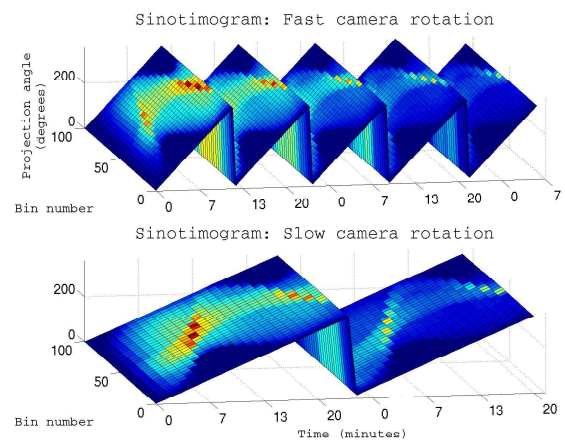


No consistent sinogram is available in dynamic SPECT. The **sinotimogram** is a way of visualizing the projections of a changing distribution. The faster the camera rotation, the more consistent the projections become. The source activity decays noticeably during the slow rotation acquisition.

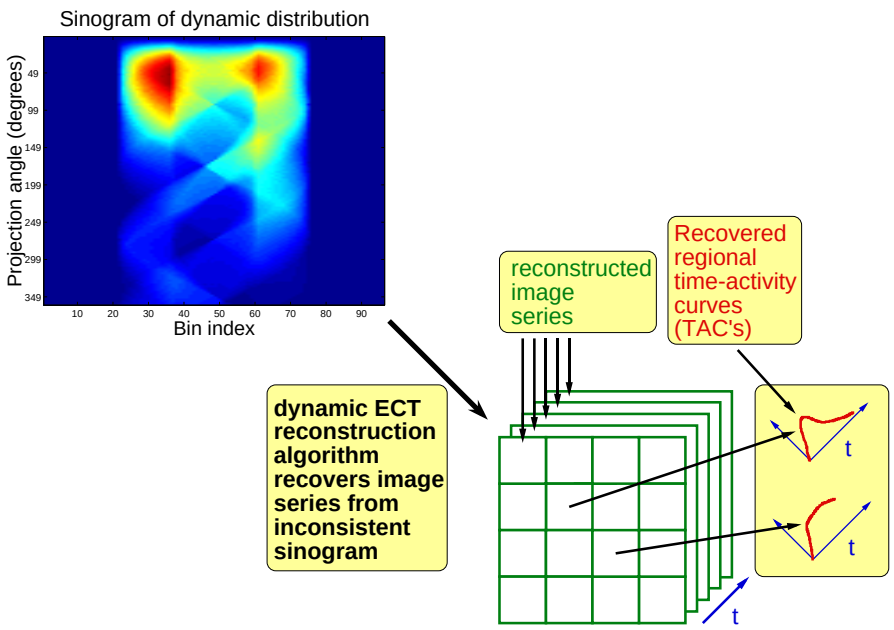




## Frontiers of SPECT: Dynamic SPECT

- In dynamic SPECT, we need to recover not only the source intensities, but their time courses. A dynamic SPECT reconstruction is a **movie** of the **time-activity curves** of each pixel.
- All SPECT is to some degree dynamic.
- In myocardial perfusion and receptor binding studies where the tracer has been designed to stick and stay put, the distribution is imaged once some of the tracer has stuck and most of the unbound tracer has washed out.
- However, sometimes the rates at which a tracer washes in and washes out yield important functional physiological parameters e.g.
  1. Fatty acid metabolism of the myocardium
  2. Rate of hormone release from a gland
  3. Rate of myocardial tracer uptake and wash-out



## Frontiers of SPECT: Dynamic SPECT

- In order to usefully solve underdetermined problems, additional information must be incorporated.
- If we can model a process, say the passage of a tracer into and out of the myocardium, we can solve for the parameters of this process rather than the pixel values at all time points.
- This incorporation of **prior knowledge reduces the problem dimension** and improves its condition.
- We will discuss **compartmental models** and show how these can be used to model tracers kinetics in living organisms.



## Frontiers of SPECT: Dynamic SPECT

- For example, $^{99m}$Tc-teboroxime is a tracer that rapidly washes in and out of the myocardium.
- Immediately after injection, the tracer appears in the blood pumped out by the left ventricle.
- It washes into the myocardium more slowly.
- In defective myocardium, less tracer washes in and wash-in occurs more slowly. Wash-out is faster than in normal myocardium.
- $^{99m}$Tc-teboroxime eventually accumulates in the liver.

**To image $^{99m}$Tc-teboroxime, we either need:**

1. A SPECT system with heads that rotate very fast.
2. A reconstruction algorithm that can accommodate data inconsistency.

## Frontiers of SPECT: Dynamic SPECT

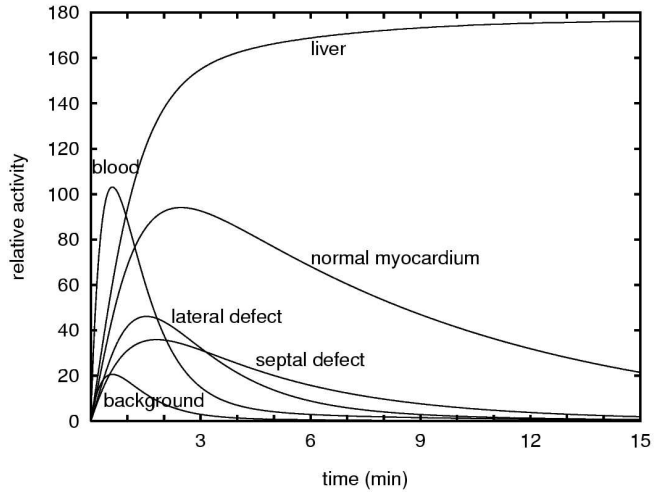


Source: Reutter et al., LBNL

TACs produced by a single compartment model of $^{99m}$Tc-teboroxime kinetics.



## Frontiers of SPECT: Dynamic SPECT

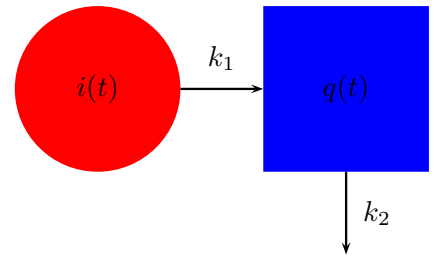


- The above diagram is a schematic representation of a **single compartment model**. It is a linear system that has $i(t)$ as the input. Since the input is an injection of tracer into the blood stream, it is called the **blood input function**.
- The amount of tracer in the myocardium is given by $q(t)$. This is the system output.



## Frontiers of SPECT: Dynamic SPECT

- The myocardium is modeled as having a permeable **membrane** separating it from the blood stream.
- The amount of tracer **entering** the myocardium is proportional to the amount in the blood $i(t)$ and the diffusion constant $k_1$ (the wash-in parameter).
- The amount of tracer leaving the myocardium is proportional to the amount in the myocardium $q(t)$ and the diffusion constant $k_2$ (the wash-out parameter). We ignore the contribution of wash-out to $i(t)$.
- The above model can be expressed as:

$$\frac{dq}{dt} = k_1\, i(t) - k_2\, q(t)$$

- Taking Laplace transforms of both sides gives:

$$s\, Q(s) = k_1\, I(s) - k_2\, Q(s)$$



## Frontiers of SPECT: Dynamic SPECT

- Rearranging yields:

$$Q(s) = \frac{k_1}{s + k_2} I(s)$$

- Applying the inverse transform, we have:

$$q(t) = i(t) * k_1\, \mathrm{e}^{-k_2 t}$$

- In dynamic SPECT, the objective of reconstruction is to find $q(t)$ for every pixel at every time point.
- Alternatively, if we simply find $k_1$ and $k_2$ for every pixel, we can calculate $q(t)$ at every time point. This is a much easier and more feasible problem.
- An optimization algorithm can be used to find those values of $k_1$ and $k_2$ that maximize the probability of obtaining a measured sinotimogram given the **projection matrix F, the attenuation map, and the kinetic model**.

## Frontiers of SPECT: Dynamic SPECT

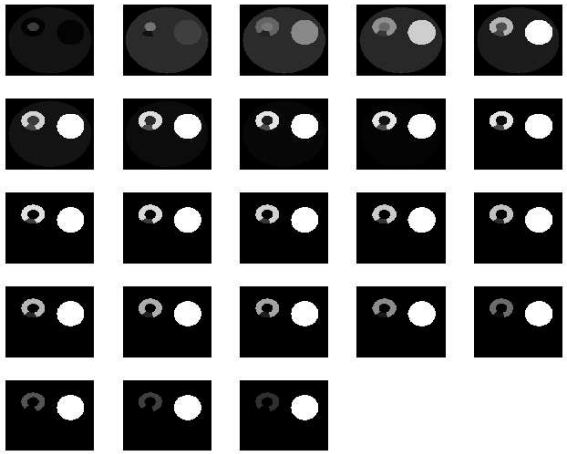

Computer generated dynamic phantom containing myocardium (normal and defect), liver and left ventricular blood pool. Images are generated at 40 second intervals.



## Frontiers of SPECT: Dynamic SPECT

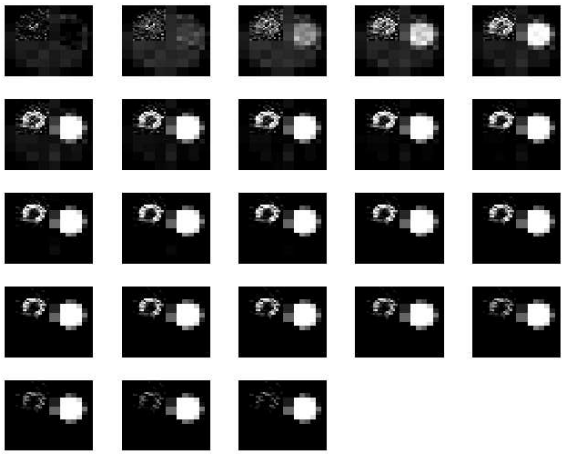

Tracer kinetic movie reconstructed using dynamic SPECT reconstruction algorithm from highly inconsistent projections in the presence of Poisson noise (500,000 total counts).



## Frontiers of SPECT: Dynamic SPECT

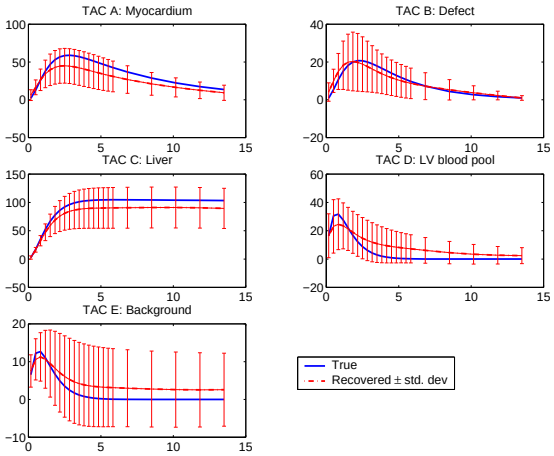


Original and reconstructed time-activity curves. Time is the given in minutes.